

Chapter IX

Molecular Docking of Triazine analogues

9.1: Introduction

Mitogen activated protein kinases (MAPK) are group of serine/threonine protein kinases that play an important role in signal transduction in many cellular process including growth, differentiation, cell death, and survival [1-5]. There are at least six different groups of MAPK that have been identified in humans cells: the extracellular signal-regulated protein kinases (ERK1, ERK2); c-Jun N-terminal kinases (JNK1, JNK2, JNK3) p38s (p38a, p38b, p38g, p38d); ERK5; ERK3s (ERK3, p97 MAPK, MAPK4); ERK7s (ERK7, ERK8) [6-8]. Each group of MAPKs can be simulated by a separate signal transduction pathway in response to different extracellular stimuli. MAP kinase plays a fundamental role to generate several diseases, such as asthma, osteoarthritis, rheumatoid arthritis, and chronic inflammatory autoimmune disease. The inhibition of MAP kinase would potentially prevent the underlying pathophysiology in the inflammatory diseases [9-11]. Rheumatoid arthritis causes damage of cartilage and deformation of bones [12]. The injury inflammation caused by inflammatory mediators such as Tumor necrosis factor- α and Interleukin-1 β [13]. Biosynthesis of these two proinflammatorycytokins regulated by p38 and these two cytokins are associated with the progression of rheumatoid arthritis [14].

Triazine derivatives show wide spectrum of biological activities in antimicrobial effect, Erm (erythromycin-resistance methylase) methyl transferase inhibition, anti-trypanosomal activity, VLA-4 (integrin very late antigen-4) antagonism, estrogen receptor modulation, cytotoxic activity [15-17]. Hexamethyl melamine, a triazine derivative possesses various pharmacological actions against breast, lung and ovarian cancers, severe adverse effect nausea, vomiting, abdominal cramps, and anorexia [18].

Leftheris et al. reported triaminotriazineamide as potent inhibitor of p38 MAPkinase [19]. Zheng et al introduced various aryl amino groups in to the triazine scaffold and determined their biological activity [20]. Taking the experimental activity from the work of “Zheng et al.” as dependent variable, we formulate a mathematical model, based on binding energy to design numbers of potent triazine scaffold-based inhibitor (Figure 1)

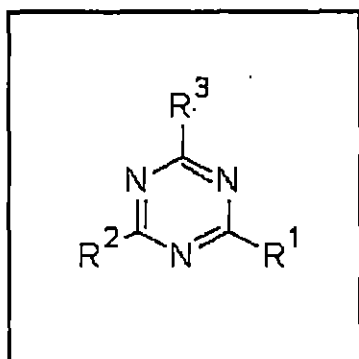


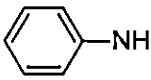
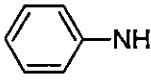
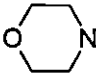
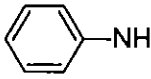
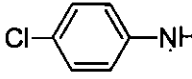
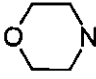
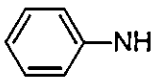
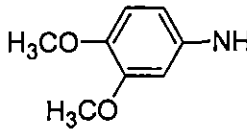
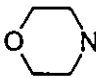
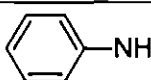
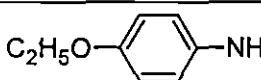
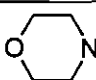
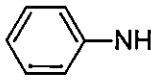
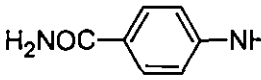
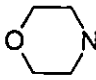
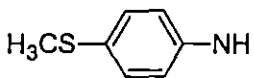
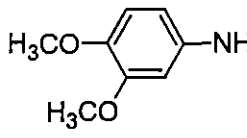
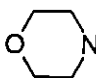
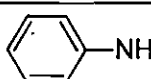
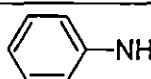
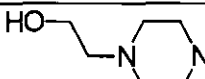
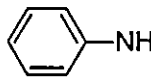
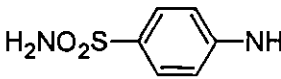
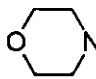
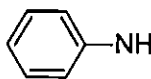
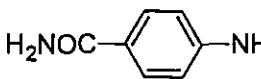
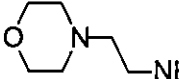
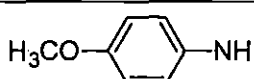
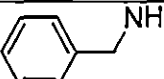
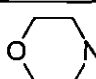
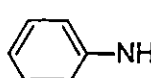
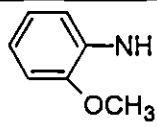
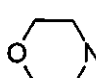
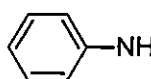
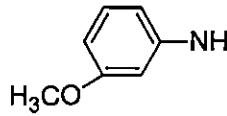
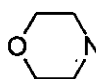
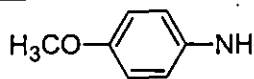
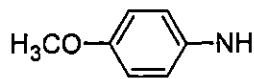
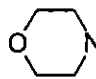
Figure 1

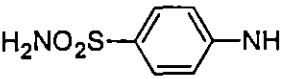
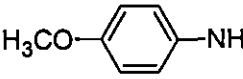
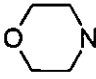
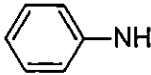
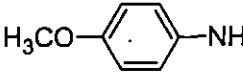
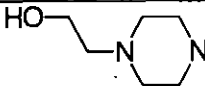
Structural representation triaminotriazine derivatives

Triazine derivatives and their corresponding inhibitory activities against HT-29 cells are shown in Table 1

Table1: Chemical structures and inhibitory activities against HT-29 cells of triazine derivatives by substituting R1, R2, R3 of T

Com	R1	R2	R3	%Inhibition at $\mu\text{M}^{\text{a}}\ln(\text{HT}29)$
1				4.3883
2				4.5053

Com	R1	R2	R3	%Inhibition at $\mu\text{M}^{\text{a}}\text{In}(\text{HT29})$
3				4.4427
4				4.4671
5				4.336
6				4.4716
7				4.4751
8				4.3994
9				4.332
10				4.387
11				4.3121
12				4.4819
13				4.492
14				4.4705
15				4.3895

Com	R1	R2	R3	%Inhibition at $\mu\text{M}^{\alpha}\ln(\text{HT29})$
16				4.4212
17				4.3477

* $\ln(\text{HT29})$ – Natural logarithm of HT29

9.2: Materials and Methods

Experimental Section

Preparation of inhibitor

Triazine inhibitors used for docking study were collected from the published work of Zheng *et al.* [20]. Using draw mode of Chemsketch the ligand molecules were drawn and three dimensional optimizations were done and then saved in mol file. For docking experiments with AutoDock 4.2, ligand molecules were optimized, and saved as in pdb format with the aid of Arguslab 4.2 [21]. Next ligand is loaded in AutoDock Tool (ADT). Gasteiger charges are added. ADT selected a root with the minimum number of rotatable branches. Root was detected. Next ligand was saved in PDBQT format. Then prepared ligand was used in docking simulation in the next step.

Preparation of protein

In the present article crystallographic structure of P38 MAP kinase was downloaded from the Protein Data Bank as PDB file (PDB entry code 1kv2) [22]. Missing atoms were repaired to the crystallographic structure of the SPDBV software package [21]. For docking simulation using Autodock all polar hydrogen was added with the GROMACS modeling package. The resulting structure was optimized by the GROMACS force field.

During minimization, the heavy atoms were kept fixed at their initial crystal coordinates by restraining. Minimization was carried out under a vacuum medium. Electrostatic interactions were calculated using the cut-off method. Finally, solvation parameters were added using the ADDSOL utility of AutoDock 4.2. Default values of atomic solvation parameters were used throughout the calculations. The grid maps of the protein were used in the docking experiments was calculated using the AutoGrid utility program.

Docking: Docking studies were performed with AutoDock4.2 using Lamarckian genetic algorithm [23]. The flexible docking procedure was used for a P38 MAP kinase protein and a flexible ligand. A grid of 94, 78, 62 points in x,y, and z direction was constructed. A grid spacing of 0.375Å and distance- dependent function of the dielectric constant was used for the calculation of the energy map. The defaults settings were used for all other parameters. The entire calculations were carried out on PC based machines running Linux as operating system. At the end of docking, ligand with most favorable free energy of binding were noted. The best conformer was chosen based on the lowest free energy of binding. The protein with the best conformer is saved as complex and analyzed using Molegro Molecular Viewer and PyMOL [24, 25].

9.3: Results and Discussion

Molecules were successfully docked on to the active site of P38 MAP according to the above docking analysis. Results of the docking experiments we calculated free energy of binding for each complex with triazine analogues and P38 MAP kinase are shown in Table 2.

Total 17 compounds were used for regression analysis. A regression equation was performed using one index, free energy of binding.

$$\ln HT29 = 4.507487 + (0.0090)bindingenergy$$

By this equation we calculated predicted ln HT29 activity (Table2).

Table 2: Actual and predicted activities of the training set molecules

Compound	Free energy of Binding (kcal/mol)	% Inhibition at $\mu\text{M}^{\alpha}\ln(\text{HT-29})$	Predicted %Inhibition at $\mu\text{M}^{\alpha}\ln(\text{HT-29})$
1	-8.34	4.3883	4.4288
2	-9.03	4.5053	4.4224
3	-8.67	4.4427	4.4258
4	-8.77	4.4671	4.4248
5	-8.9	4.336	4.4236
6	-6.95	4.4716	4.4418
7	-8.18	4.4751	4.4303
8	-8.67	4.3994	4.4258
9	-19	4.332	4.3297
10	-8.88	4.387	4.4238
11	-9.74	4.3121	4.4158
12	-9.44	4.4819	4.4186
13	-9.32	4.492	4.41972
14	-9.15	4.4705	4.4213
15	-9.11	4.3895	4.4217
16	-9.66	4.4212	4.4166
17	-8.33	4.3477	4.4289

Docking results shows all triazine inhibitors docked in to allosteric of P38 MAP kinase and their calculated free energy of binding is shown in table1. From the table it is shown that lowest binding energy value is obtained for compound 11. Docking structure of compound11 is presented in Figure 2. A repressive figure containing the inhibitor (11) in the binding site of P38 MAP kinase is presented in Figure 3. From the Figure 3, it is clear that the inhibitor is well inside binding cavity.

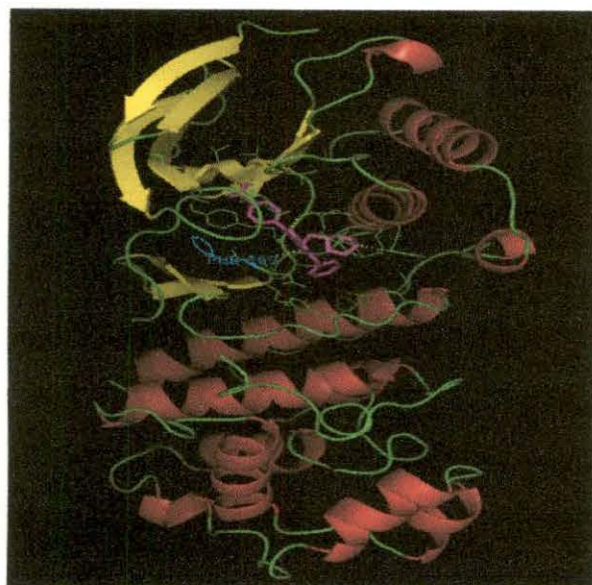


Figure 2: Compound 11 in a binding pocket of P38 MAP. The inhibitor show in stick model (magenta)

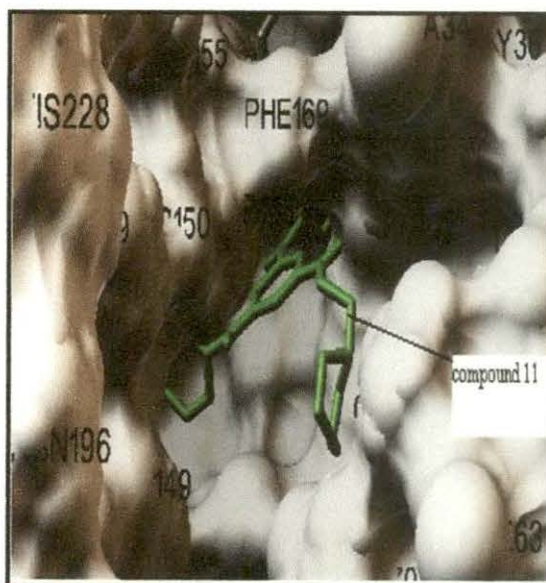


Figure 3: Docking result of triazine inhibitor (11)

Figure 4 shows ligand was surrounded by both polar and apolar hydrophobic group such as ARG67, ARG70, GLU71, LYS53, VAL38, GLU71, PHE169, ASP168, HIS148, LEU7, LEU75, ILE84, ILE166, ILE41. These amino acid residues stabilized both polar and apolar parts of ligands. Figure shows the four hydrogen bond interaction observed between inhibitor and P38 MAP kinase.

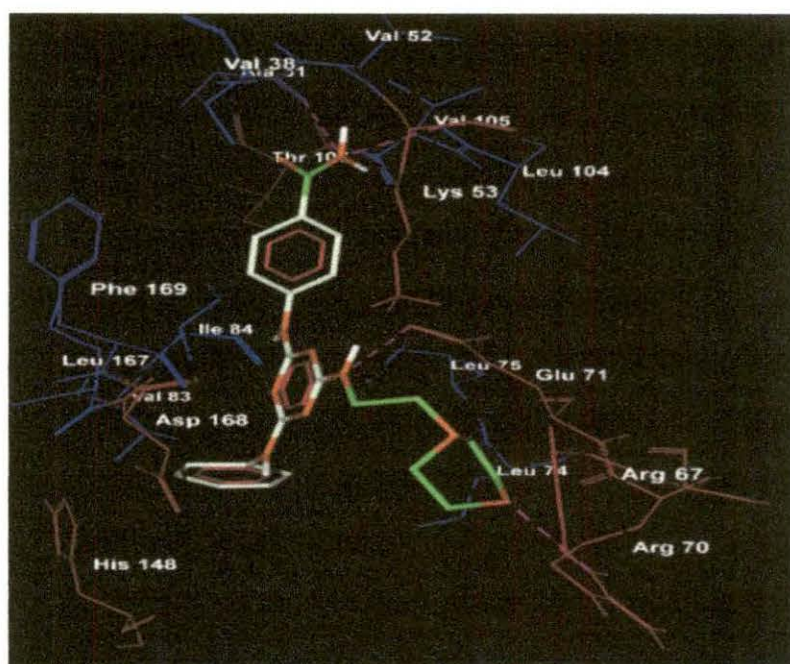


Figure 4: Docking result of compound11 in the active site of p38 MAP kinase. The inhibitor presented by stick mode (Green is hydrophobic part and orange is hydrophilic part) and important residues in the active site of the enzyme are presented by wireframe.

It is seen that presence of one morpolino or anilino ring is essential for the activity of triazine derivatives. Also introduced pyrimidine ring in triazine scaffold gives very high predicted activity. Basis of this finding we designed several triazine analogues as more potent p38 MAP kinase inhibitors and Docking simulation was performed. Structures of Triazine analogue and their corresponding binding energy are shown in Table 3.

Table 3: Chemical structures of designed triazine derivatives by substituting R1, R2, R3 of E and their Docking energies

Compound	R1	R2	R3	Binding Energy (kcal/mol)
1a				-8.75
1b				-7.96
1c				-9.03
1d				-9.07
1e				-8.51
1f				-9.29
1h				-8.83
1i				-9.40

Compound	R1	R2	R3	Binding Energy (kcal/mol)
1j				-9.31
1k				-9.30
1l				-9.36
1m				-8.1
1n				-9.26
1o				-8.15
1p				-7.13
1q				-8.0

Docking analysis also performed for the design triazine inhibitors and inhibitors are docked in to allosteric site of P38 MAP. Their calculated free energy of binding is shown in table 3. From the table it is shown that lowest binding energy value is obtained for lowest binding energy value is obtained for designed compound 1i. Docking structure of compound 1i is presented in Figure 5. One of the designed compound (1i) docked with p38 MAP kinase is presented in Figure 6. It is observed that designed compound is also inside the binding cavity (Figure 6).

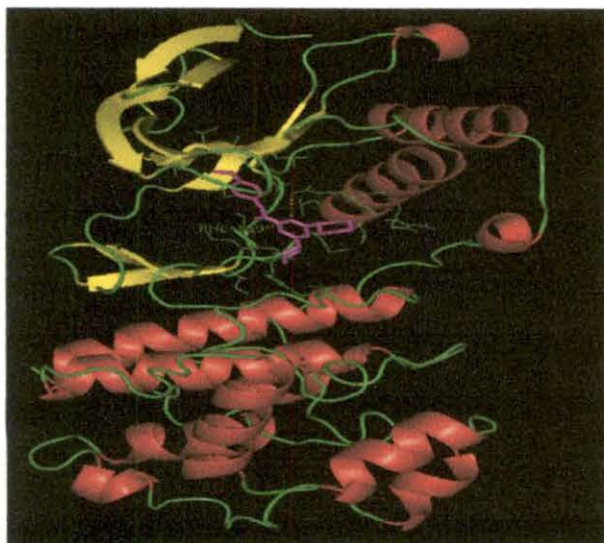


Figure 5: Compound 11 in a binding pocket of P38 MAP. The inhibitor show in stick model (magenta)

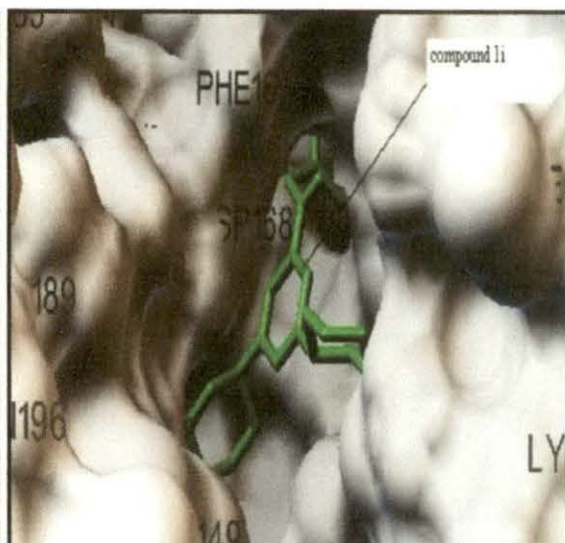


Figure 6: Docking result of triazin inhibitor (1i)

Figure 7 shows ligand was surrounded by both polar and apolar hydrophobic group such as Glu71, LYS 53, VAL52, ALA51, PHE169, ASP168, HIS148, LEU75, LEU67, VAL83, ILE84, MET78. These amino acid residues stabilized both polar and apolar parts of ligands,

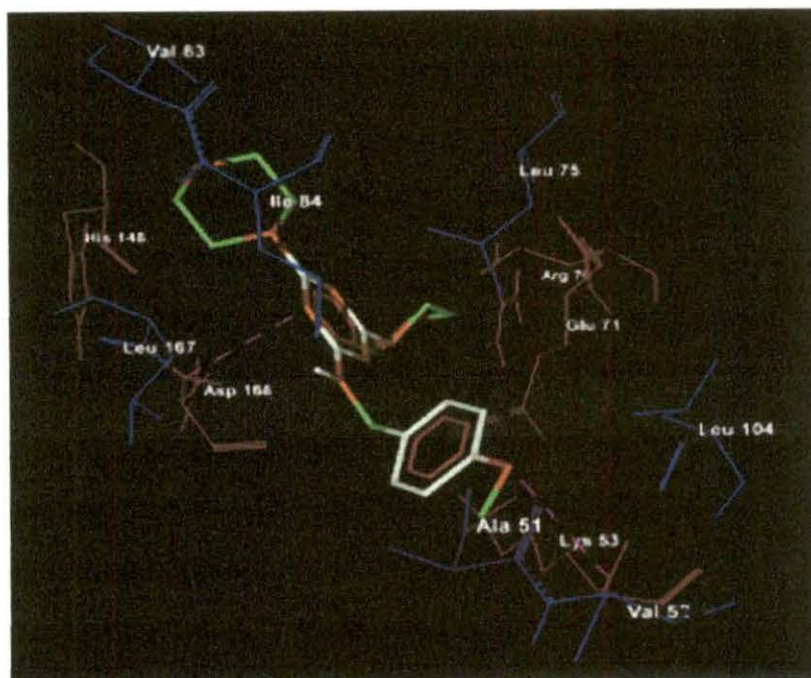


Figure 7: Docking pose of compound 11 in the active site of p38 MAP kinase. The inhibitor presented by stick mode (Green is hydrophobic part and orange is

hydrophilic part) and important residues in the active site of the enzyme are presented by wireframe.

9.4: References

1. Whitmarsh AJ, Davis RJ (1996) *J. Mol. Med.*, **74**: 589- 607.
2. Garrington TP, Johnson GL (1999) *Curr. Opin. Cell Biol.*, **11**: 211-218.
3. Cohen, P. The search for physiological substrates of MAP and SAP kinases in mammalian cells. *Trends. Cell Biol.* **1997**, *7*: 353–361.
4. Ip, Y.T., and R.J. Davis. Signal transduction by the c-Jun N-terminal kinase.(JNK): from inflammation to *development*. *Curr. Opin. Cell Biol.* **1998**, *10*:205–219.
5. Davis, R.J... Signal transduction by the c-Jun N-terminal kinase (JNK): from inflammation to development. *Curr. Opin. Cell Biol.* **1998**, *10*: 205–219.
6. GonzalezFA, Raden D, Rigby MR, Davis RJ (1992) Heterogeneous expression of four MAP kinase isoforms in human tissues. *FEBS Lett.*,**1992**, *304*, 170-178.
7. Mandlekar S, Kong AN (2001) Mechanisms of tamoxifen-induced apoptosis. *Apoptosis*.**6**: 469-77.
8. Kant S, Schumacher S, Singh MK, Kispert A, kotlarov A (2006) *Biol Chem.*, **281**: 355111-355119.
9. Choy EHS, Panayi GS (2001) Mechanisms of Disease: Cytokine Pathways and Joint Inflammation in Rheumatoid Arthritis. *N Eng J Med.*, **344**: 907-916.

10. Dinarello CA (1991) Inflammatory cytokines: interleukin-1 and tumor necrosis factor as effector molecules in autoimmune diseases. *Curr Opin Immunol.* 3: 941-948.
11. Palladino MA, Bahjat FR, Theodorakis EA, Moldawer LL (2003) Anti-TNF-alpha therapies: the next generation. *Nat Rev Drug Disc.*, 2: 736-741.
12. Chen E, Keystone EC, Fish EN (1993) *Arthritis and Rheum.*, 36:901-910.
13. Salituro FG, Germann UA, Wilson KP, Bemis GW, Fox T, et al. (1999) *Curr Med Chem.*, 6, 807-823
14. Harada J, Sugimoto M (1999) *Japan J Pharmacol.*, 79: 369-378.
15. Silen JL, Lu AT, Solas DW, Gore MA, Maclean D (1998) Screening for Novel Antimicrobials from Encoded Combinatorial Libraries by Using a Two-Dimensional Agar Format. *Antimicrob. Agents Chemother.* 42, 1447.
16. Klenke B, Stewart M, Barrett MP, Brun R, Gilbert IH (2001) *J. Med. Chem.*, 44: 3440.
17. Menicagli R, Samaritani S, Signore G, Vaglini F, Via LD (2004) *J. Med. Chem.*, 47: 4649.
18. Foster BJ, Harding BJ, Leyland JB, Hoth D (1986) *Cancer Treat. Rev.*, 8: 197.
19. Leftheris K, Ahamed G, Chan R, Dyckman AJ, Hussain Z (2004) The discovery of orally active triaminotriazine aniline amides as inhibitors of p38 MAP kinase. *J. Med. Chem.*, 47: 6283.

20. Zheng M, Xu C, Ma J, Sun Y, Du F, et al. (2007) Synthesis and antitumor evaluation of a novel series of triaminotriazine derivatives. *Bioorganic & Medicinal Chemistry*. 15: 1815-1827.
21. <http://www.seanet.com/~mthompson/Arguslab>.
22. Pargellis C, Gilmore L, Graham AG, Grob PM, Hickey ER (2002) Inhibition of P38 Map-Kinase by utilizing a Novel Allosteric Binding State. *J Regan Nat. Struct. Biol.*, 9: 268-272.
23. Morris GM, Goodsell DS, Halliday RS, Huey R, Hart WE, et al. (1998) Automated Docking Using a Lamarckian Genetic Algorithm and Empirical Binding Free Energy Function. *J. Comput. Chem.*, 19: 1639-1662.
24. Molegro Molecular Viewer (MMV), 2008. 1.0, Molegro, Denmark.
25. Delano WL (2002) The PyMOL Molecular Graphics System.